5.1 Introduction

The refractory castable generally contains two different constituents, i.e., the major part is non-continuous refractory grade aggregates, and another part is a continuous matrix or bonding phase. The interactions between these two constituents regulate the final properties of the castables. Therefore, the selection of the bonding or matrix phase, which is greatly affected the product characteristics, is highly sensitive for making the refractory castable. The binder phase delivers both strengths at a green body and at higher temperatures by forming high temperature phases or by enhancing the sintering kinetics through the decomposition on heating (Lee *et al.*, 2001; Singh and Sarkar, 2017).

Generally, the binder used in refractory castable is calcium alumina cement (CAC). However, it has some limitations, like the formation of low melting eutectic phases through the reaction of CaO with SiO_2 and Al_2O_3, for high temperature (>1500°C) applications. It degrades the corrosion resistance and high temperature mechanical strength of the castable (Parr *et al.*, 2005; Khezrabad *et al.*, 2013). So, the focuses of the researchers have now been shifted to the no cement bonding or matrix systems for high temperature applications (Khezrabad *et al.*, 2013; Lopes *et al.*, 2017; Luza *et al.*, 2018; Roy *et al.*, 2019). Recently, colloidal silica, sol-gel derived sol or fumes silica, and other micro fine or nano silica sources have been played an important role as an alternative of CAC in the castable (Khezrabad *et al.*, 2013; Luz *et al.*, 2018; Montes *et al.*, 2018; Roy *et al.*, 2019). The addition of silica sol in the refractory castables has some advantages like less or no water requirement, short mixing time, high drying rate, high permeability, low spalling risk, and introduced sustainable green strength by gelation mechanism (Ismael *et al.*, 2006; 2008). Furthermore, the nano-size reactive silica containing sol may endorse the formation of mullite ($3Al_2O_3 \cdot 2SiO_2$) in alumina containing refractory castables after firing (Singh and Sarkar, 2017; Luz *et al.*, 2018; Montes *et al.*, 2018). The presence of the mullite matrix phase in the castable helps to improve the various properties such as high temperature stability, chemical stability, low thermal expansion, high refractoriness, good strength, and toughness of the refractory (Schneider *et*

al., 2008). Therefore, colloidal or fumes silica is commercially exploited as an alternative refractory binding system and it is expected to increase the demands in the near future. Consequently, the preparation of these nano-size precursors is difficult and expensive. It affects the cost of the final products. To develop a facile, sustainable and economical route for the preparation of nano silica containing sources is challenging for the researchers. Lim *et al.* (2010) have described the several synthesis methods, i.e., hydrolysis and condensation of silicate compound, direct oxidation of silicon, and ion exchange of sodium silicate, for the preparation of colloidal silica. Hyde *et al.* (2016) have provided an overview about the up-to-date laboratory and industrial-based colloidal, fumes and nano silica synthesis routes. Each of the process retains its own advantages and limitations according to the commercialization and tailor properties of the product. Rice husk (RH) or waste rice husk ash (RHA) derived silica sol or nano silica can also be used as an alternative silica source for refractory castables. Sembiring *et al.* (2014) have prepared mullite ceramic from RHA derived silica. Serra *et al.* (2016) have revealed a reaction-sintering technique for the formation of mullite from RHA. Fernandes and Salomão (2018) have disclosed that the RHA or RH derived silica with calcined alumina has formed in-situ mullite formation.

The present study is explored a novel approach to investigate the feasibility of using RHA derived silica sol as a binder system for high alumina refractory castable. Alkali extraction method is adopted for the synthesis of silica sol from RHA. Additionally, mullite formation ability of this waste derived sol with reactive alumina is systematically investigated. Highlighting is given to the in-situ mullite formation and the physico-mechanical properties of the synthesized castables. The corrosion behavior with the blast furnace slag (BFS) at 1500°C is also discussed. The obtained properties of the in-situ mullite matrix containing castable are compared with the commercially available different silica containing high alumina refractory castable systems.

[70]

5.2 Experimental procedure

5.2.1 30 wt.% solid containing sol synthesis

The sol extraction process is similar to the previously described nano silica preparation and 7.5 wt.% solid containing sol extraction processes, as described in the chapter 4. However, more drying time was required for 30 wt.% solid containing sol than 7.5 wt.% solid containing sol.
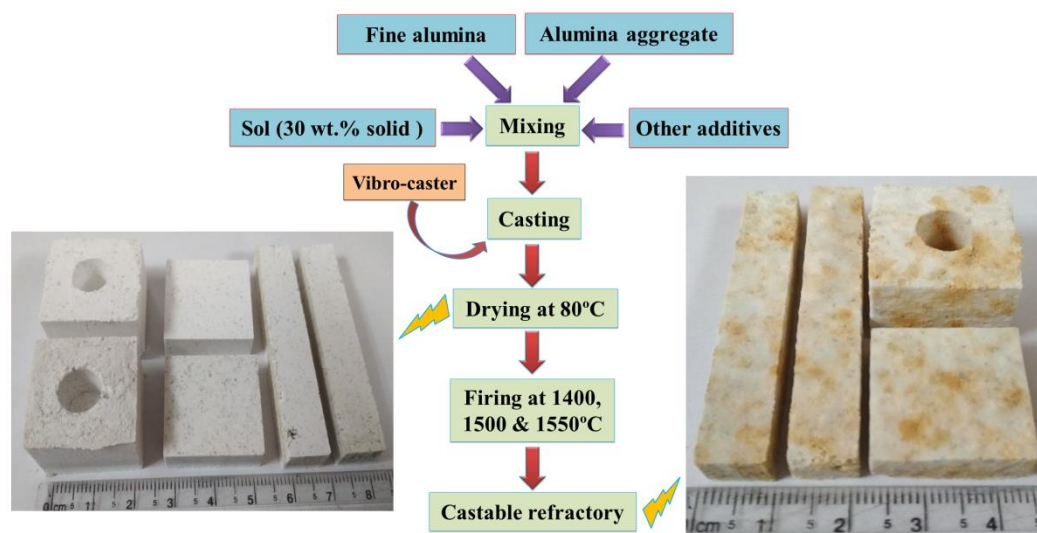
Figure 5.1 Preparation scheme of RHA derived sol and high alumina refractory castable.

5.2.2 Castable making

Figure 5.1 depicts the preparation flow chart for high alumina castable specimens. Five different castable compositions were prepared by mixing brown tabular alumina as aggregates (different sizes), calcined alumina, reactive alumina, CAC, silica sol, and a small amount of sodium hexametaphosphate (SHMP), as a dispersant agent. The composition of the different samples and the size distribution of the ingredients are depicted in Table 5.1. The c-0 composition was prepared by CAC binding system. Whereas, c-1 composition was fabricated by partially replacing CAC by the silica sol. The c-2 samples onwards compositions were made by the addition of silica sol and dry silica sol (to avoid excessive water in the castable) in the place of CAC. The last two (c-3 and c-4) compositions were prepared by the addition of dry silica sol in place of calcined alumina. Initially, SHMP, reactive alumina, calcined alumina, and both silica sol or CAC were mixed for 10 min and then aggregates, i.e., different

fraction (for good packing efficiency of castable) of brown tabular alumina were added and mixed for another 10 min. Different shapes of castable specimens were prepared by the pouring of mixed mass into different sizes ($25\times25\times10$ mm^3 and $50\times10\times10$ mm^3 rectangular, 25 mm^3 cube) properly oiled steel moulds. For better compactness, the mix filled moulds were casted by the vibro-caster for 5 min. The cement containing (c-0 and c-1) samples were released from the moulds after 2 h of casting for development of workable hardening and then the samples were cured in a ~80% relative humidity containing humidity chamber for about 24 h at room temperature to complete hydration reactions. On the other hand, sol containing castable samples (c-2, c-3 and c-4) was carefully released from the moulds after the casting without any soaking. It did not require any separate hardening and curing stages due to instant sustainable strength, which was developed through the coagulation (the water from the sol was started to absorb by the other dry aggregates during casting process and helped to decrease the inter-particle separation distance of sol nano particles with increasing the particle collision) of sol containing nano particles (Ismael *et al*., 2006). Later, all the casted specimens were carefully transferred into an air dryer to dry at 80°C for 2 h. Sintering was performed in a muffle furnace at 1400, 1500, and 1550°C for 4 h with a heating and cooling rate of 2°C/min to yield the castable refractories.

Table 5.1 Sample's nomenclature and composition for castable refractory.

Samples	Tabular alumina (wt.%)			Calcined alumina (wt.%), (<2 µm)	Reactive alumina (wt.%), (<1 µm)	CAC (wt.%), (<9 µm)	Silica sol (present SiO$_2$, wt.%)	Dry sol (wt.%)	SHMP (wt.%)	Water (wt.%)
	(1-3 mm)	(0.1-1 mm)	(<0.1 mm)							
c-0	30	20	20	9.8	16	4	0	0	0.2	5
c-1	30	20	20	9.8	16	2	2	0	0.2	2
c-2	30	20	20	9.8	16	0	3	1	0.2	0
c-3	30	20	20	8.8	16	0	3	2	0.2	0
c-4	30	20	20	7.8	16	0	3	3	0.2	0

5.3 Results and discussion
5.3.1 Characterization of 30 wt.% solid containing sol

The sol retained around 30 wt.% of solid particles after heat-treating at 1200°C. The detailed discussion about the sol and dry sol is described previously in chapter 4. The estimated cost of 30 wt.% solid (~22 nm average silica particles) containing sol is around 9.35$ per litre. It is illustrated in Table 5.2.

**Table 5.2** Cost estimation of silica sol (~30 % solid) synthesis per litre using RHA as source.

Raw materials used			Energy			Labour cost + others
Name	**Cost per kg**	**Unit price** *	**Name**	**Cost per kg**	**Unit price**	
Rice husk ash	0	0	Magnetic stirring and oven	(0.18+0.18) $	0.15 $ per KW	cost + others
NaOH pellet	2.94 $	5.2 $ per kg				
HCl solution (1N)	4.05 $	5.4 $ per L				
	6.99 $			0.36 $		2 $
Total extraction cost of silica sol per litre ~ 9.35 $						

* https://www.lobachemie.com/flipbooks

5.3.2 Characterization of castable

The castable samples with different compositions were prepared using RHA derived sol as a binder, and ten specimens of each composition were fabricated for appropriate results. The samples were sintered at 1400°C, 1500°C, and 1550°C. These temperatures are lower than the sintering temperature of conventional no cement castable (Singh and Sarkar, (2016); (2016b)). No deformity on shape and dimensions was detected for all the sintered castable samples, as exhibits in Figure 5.1.

The phase analysis of refractory castable is important to identify the existence of any low melting impurity phase in the matrix of castable. It commonly deteriorates the properties and performance at high temperatures. Figure 5.2 depicts the XRD patterns of some selective sintered castable specimens. It can be identified that the corundum is a major crystalline phase for all the fired samples. However, some calcium aluminum oxide phases were identified in the XRD pattern (Figure 5.2) of c-0 samples. On the other hand, RHA derived silica sol containing samples (c-2, c-3 and c-4) are retained some in-situ mullite peaks in the XRD pattern (Figure 5.2) as a minor phase. This mullite is developed through the diffusion reaction of reactive alumina and sol containing nano silica at above 1200°C, as discussed in the previous chapter 4. Theoretically, 2 wt.% (c-1), 4 wt.% (c-2), 5 wt.% (c-3) and 6 wt.% (c-4) nano silica containing high alumina castable are produced maximum 7.10 wt.%, 14.20 wt.%, 17.75 wt.% and 21.30 wt.% in-situ mullite ($3Al_2O_3·2SiO_2$), respectively, in the matrix. Moreover, some unreacted silica peaks are detected in 6 wt.% of nano silica containing (c-4) castable specimens. So, further addition of silica sol in the composition of castable may dilute the high temperature properties due to the unreacted of free silica in the matrix.

[73]
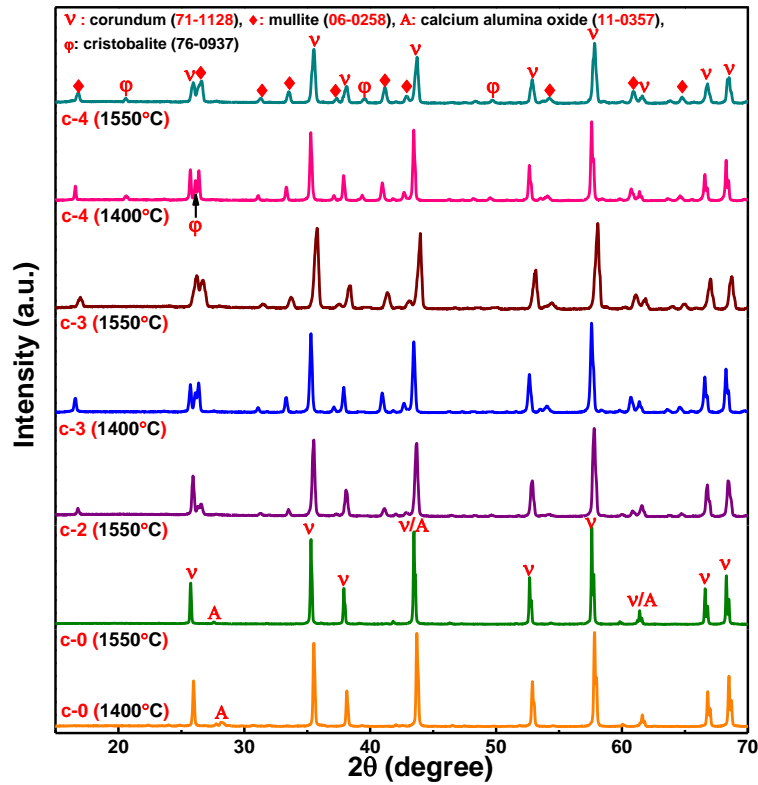
Figure 5.2 XRD patterns of sintered castable specimens.

The behaviors of the sintered ceramic bodies are not only influenced by the present phase but also very much dependent on the developed microstructure like distribution of present phases, sinterability, and amount of pores (Ghosh *et al*., 2003). The SEM images of the fractured cross-sectional surfaces of the sintered castable (c-0 and c-3) specimens are depicted in Figure 5.3. The cement containing (c-0) and sol containing (c-3) specimens demonstrated slightly different microstructures. c-0 specimen showed a lower grade of densification with some pores on the surface at 1400°C. However, at 1550°C sintered c-0 specimen exhibited a compacted structure without any magnificent pores. High magnification image of c-0 (1550°C) sample showed some liquid phases in the interfaces of corundum grains. Hence, liquid phase sintering is attributed to CAC containing samples. Conversely, sol containing c-3 specimens retained a uniform, compact morphology. It may be ascribed due to the sol with nano silica particles. It has great sinterability characteristic at high temperature due to the high surface area of nano silica particles. It helps to react with alumina sources and forms a continuous in-situ mullite matrix. The needle like mullite grains are formed in the

[74]

castable network, as observed in the high magnification image. At high temperatures, more activation energy may help grow the mullite grains in a particular direction.
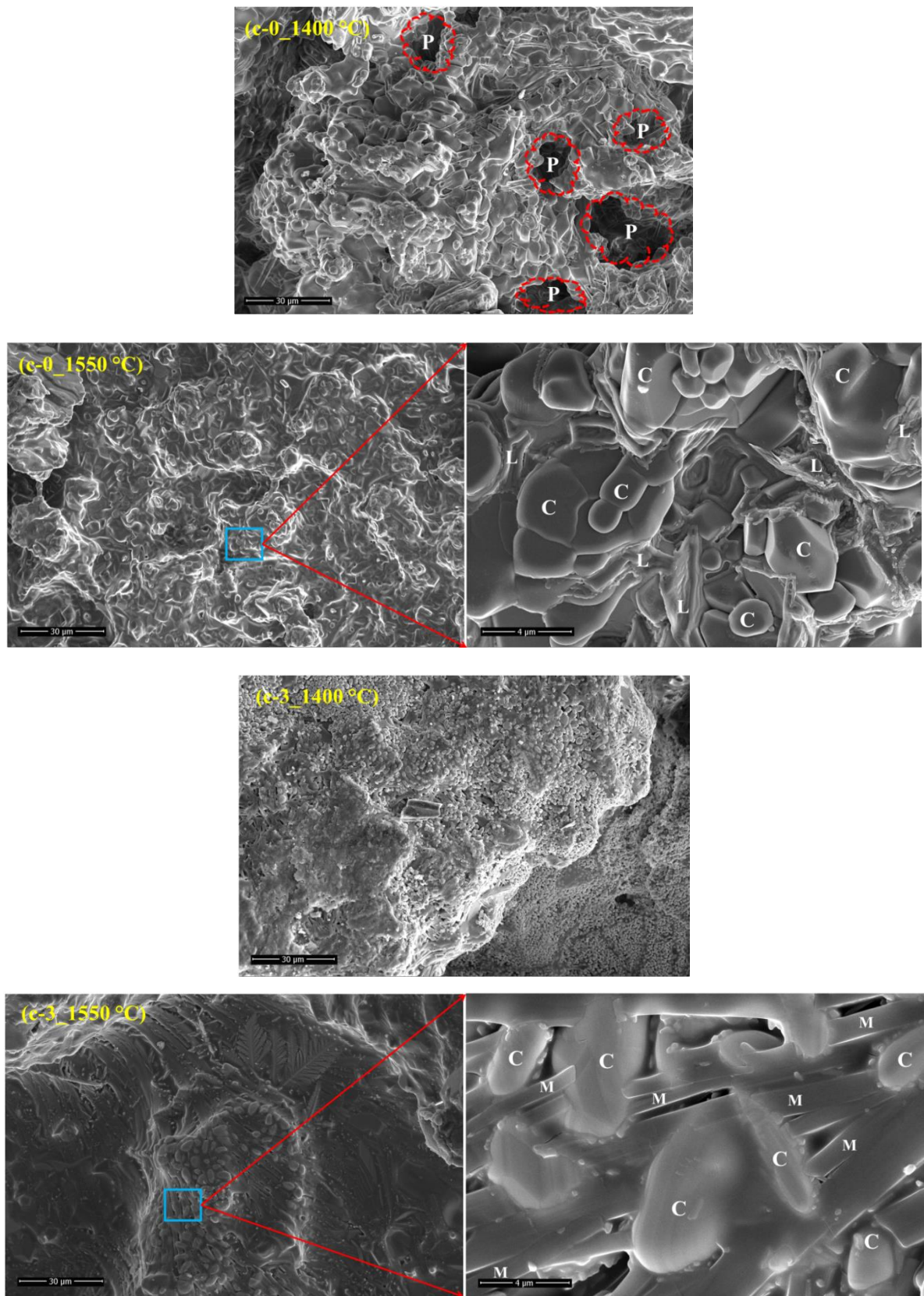
Figure 5.3 SEM micrographs of the fractured cross sectional surfaces of sintered refractory castables (P: pore, M: mullite, C: corundum, L: liquid).

Table 5.3 depicts the mean value of BD and AP of the fired castable specimens. It can be observed that the RHA derived sol containing samples show a slight lower value of AP than CAC containing c-0 sample sintered at 1400°C. Sol containing nano silica is started to form a significant amount in-situ mullite phase after 1250°C in the castable (chapter 4). It enhances the sintering kinetics through the developing of continuous bonding matrix in the aggregates. Additionally, nano particles improved the packing efficiency of refractory castable by filling inter-aggregates pores of castable (Roy *et al.*, 2019). 6 wt.% (3 wt.% sol + 3 wt.% dry sol) silica containing c-4 sample exhibits the lowest porosity. It may be ascribed due to the presence of unreacted nano silica at 1400°C (Figure 5.2). This free nano silica formed a viscous phase in-between the refractory aggregates and filled the pores. However, the porosity effect did not significantly affect the BD of the castable. It may be due to high density CAC (~3340 kg/m^3) is replaced by the low density material (silica, ~2200kg/m^3) or formation of low density phase i.e. mullite (~3100kg/m^3). The AP values are reduced and BD is improved with increasing the sintering temperature from 1400°C to 1500°C or 1550°C due to accelerate different sintering mechanism and shrinking of pores volume. c-0 sample shows more reduction of AP value with increasing the firing temperature from 1400°C to 1550°C. It may be attributed due to the formation of low eutectic phases above 1400°C (Figure 5.3). This phases introduced the liquid phase sintering in the castable (c-0 and c-1) and reduced the AP values.

Table 5.3 Apparent porosity and bulk density of sintered castable samples.

Samples	Apparent porosity (%)						Bulk density (gm/cc)					
	1400°C		1500°C		1550°C		1400°C		1500°C		1550°C	
	Mean	s.d.	Mean	s.d.	Mean	s.d.	Mean	s.d.	Mean	s.d.	Mean	s.d.
c-0	17.78	1.02	10.95	0.68	7.61	0.54	2.73	0.02	2.83	0.04	2.90	0.03
c-1	15.17	0.95	11.27	0.83	7.57	0.62	2.75	0.02	2.82	0.04	2.91	0.05
c-2	14.27	0.79	10.08	0.66	7.22	0.74	2.76	0.03	2.81	0.03	2.92	0.04
c-3	13.11	0.92	8.75	0.78	6.49	0.45	2.77	0.03	2.82	0.03	2.91	0.03
c-4	10.43	0.86	7.23	0.84	5.41	0.53	2.76	0.03	2.84	0.04	2.93	0.04

The green CCS values of the castable specimens after drying at 80°C are shown in Figure 5.4 (a). CAC containing samples (c-0 and c-1) show good green strength than sol

containing samples (c-2, c-3 and c-4). It may be happened due to the formation of CAH_{10}, C_3AH_6 and C_2AH_8 phases in the castable matrix through the hydration of CAC containing phases like CA, CA_2 and $C_{12}A_7$ (Mor *et al.*, 2017). These hydration phases provided an interlocked network in the system of castable and helped to bind the aggregates. It delivers the green strength or setting behavior of the castable. However, sol containing specimens also displayed the sustainable strength values. The sol retains hydrated silicon (Si-OH) particles. During drying of castable, the hydroxyl group from the sol is removed as a water vapors and free silanol groups (Si-OH) is transferred into siloxane bond (Si-O-Si) through the equation no. 5.1. It forms 3D networks of Si-O-Si bonds in the castable matrix. It can be encapsulated the solid aggregates and provided the green strength of the castable. Figure 5.4(b) depicts the schematic representation of gelation mechanisms of nano silica sol. It helps to understand the reason behind the green strength of sol containing castable specimens.

$$-Si-OH+OH-Si- = -Si-O-Si-+H-O-H \uparrow \qquad (5.1)$$
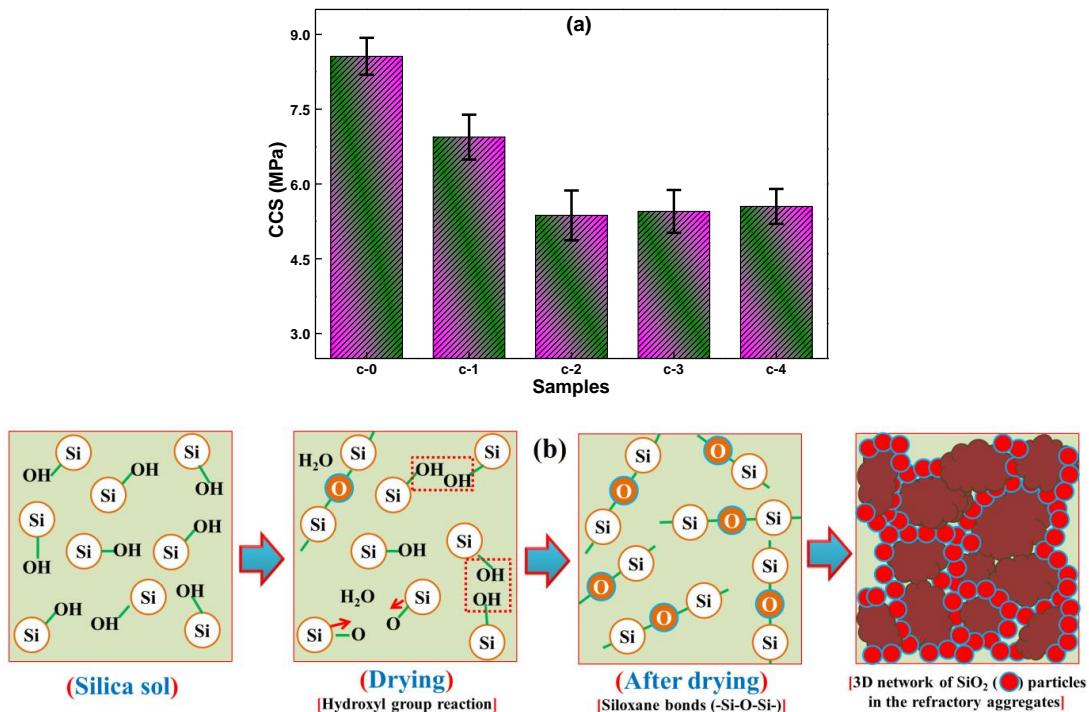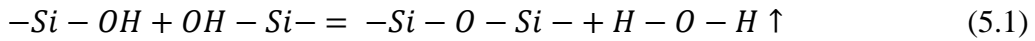
Figure 5.4 (a) Green CCS values of castable specimens after drying at 80°C and (b) gelation mechanisms of nano silica sol [10].

Figure 5.5(a-b) illustrates the CCS and bending strength (BS) values of castable specimens after sintering, respectively. The strength values of the castable specimens are

improved with the sintering temperature. It may be attributed due to the hydration or week sol bonds are substituted through the robust ceramic bonds. Subsequently, both strength values of BS and CCS are expressively improved with the addition of sol in the place of CAC (c-1 and c-2) or calcined alumina (c-3 and c-4). Sol introduces nano silica in the system, and fills the inter-aggregate void. Sol generates highly active SiO_2 particles, which are favorable to the reaction with reactive alumina for the formation of in-situ mullite. This mullite phase introduces a network into the castable matrix. The reduction of void volume and introduction of mullite network enhances the strength values of the castable with sol incorporation in the system. However, CCS and BS are improved with increasing the sintering temperature due to increase in sinterability characteristics of the castable. It is also observed that the presence of free silica in c-4 sample does not degrade the room temperature strength values.
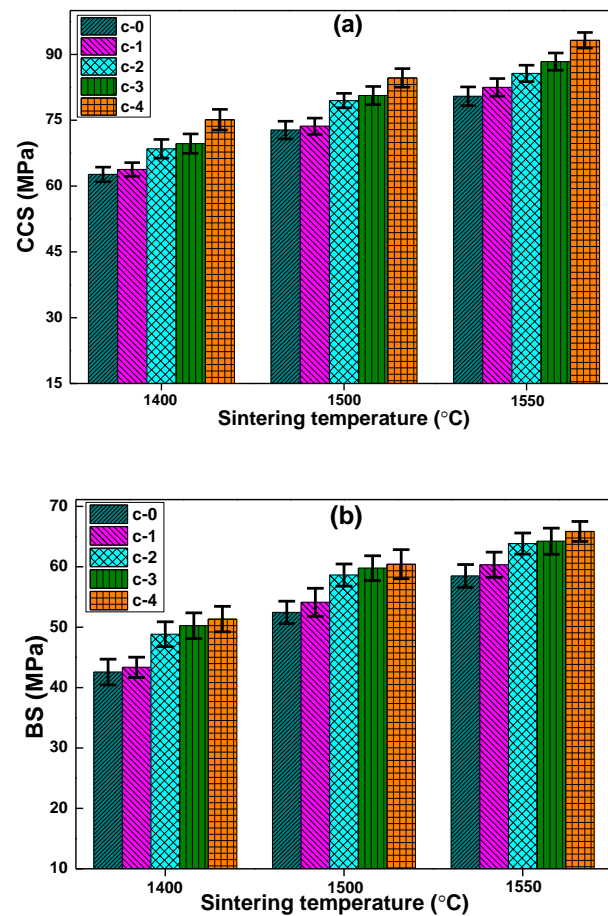
Figure 5.5 (a) CCS and (b) BS values of sintered castable specimens.

The analysis of hot flexural strength of castable specimens was performed at 1400°C. The HMoR values of some selective castable specimens (c-0, c-2, c-3 and c-4) sintered at 1400°C and 1550°C are illustrated in Figure 5.6. 1400°C sintered specimens show low value of HMoR, it may be due to lack of densification (Table 5.3). The porosity in the castable introduces number of crack generate sites, which aid to reduce the strength value. However, 1550°C sintered samples show above 10 MPa of HMoR values, which is considered for application in castable refractories (Braulio *et al.*, 2012). The development of uniform dense microstructure may be the reason of improving HMoR values. Subsequently, silica sol containing specimens exhibited higher values of HMoR due to introduce of fine mullite particles in the castable matrix. The formation of mullite is enhanced the sintering mechanisms and developed strength. The mullite (melting point ~1840°C) has higher ability to resist the braking forces than calcium aluminate phases at high temperature. The CAC containing specimens have a possibility to form low melting phase like $C_{12}A_7$ (~1400°C) in the castable system. Consequently, 6 wt.% (c-4) sol containing castable specimen shows slightly lower value of HMoR than 5 wt.% (c-3) containing specimen. It may be happened due to the presence of free nano silica, which may form viscous phases at high temperature and reduce the HMoR value of the castable.

4 wt.% CAC containing (c-0) and 5 wt.% silica containing (c-3) samples (highest HMoR among all sol containing samples) were taken for TSR evaluation. Figure 5.7 displays the percent of retention CCS values of the respective samples as a function of undergoing number of thermal cycles. The c-0 specimen showed a gradual degradation of CCS values with the thermal fatigue. It may be due to the generation of subcritical cracks in the castable system during thermal cycle because of huge temperature differences (~1170°C) and the cracks continuous propagate with repetitively thermal shock (Hasselman, 1969). The retaining strength of c-0 sample is ~59% of its original strength value after 10th thermal cycles. The silica sol containing c-3 sample initially showed a slightly higher degradation rate than c-0

sample. The mismatch of thermal expansion coefficient between alumina ($\sim 8.1 \times 10^{-6}/°C$) and mullite ($\sim 5.4 \times 10^{-6}/°C$) particles, introduces a higher concentration of stresses in the system. It aids to generate number of micro-cracks; results crack propagation in the matrix. Figure 5.8 depicts the surface morphology of c-3 specimen after 6th thermal shock cycles and it shows that the numbers of micro cracks are generated on the surface. This may be the reason of rapid reduction in the strength retainment capacity of c-3 sample. However, the strength degradation rate of c-3 is decreased after 6th thermal cycles and after 10th cycles it is retained around ~ 57 % of its initial strength value.
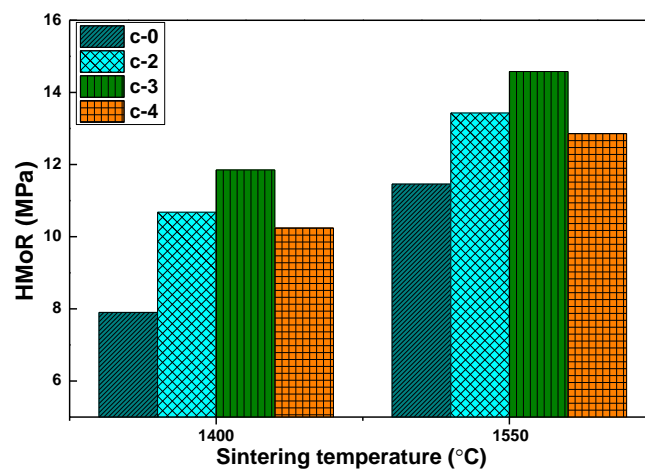

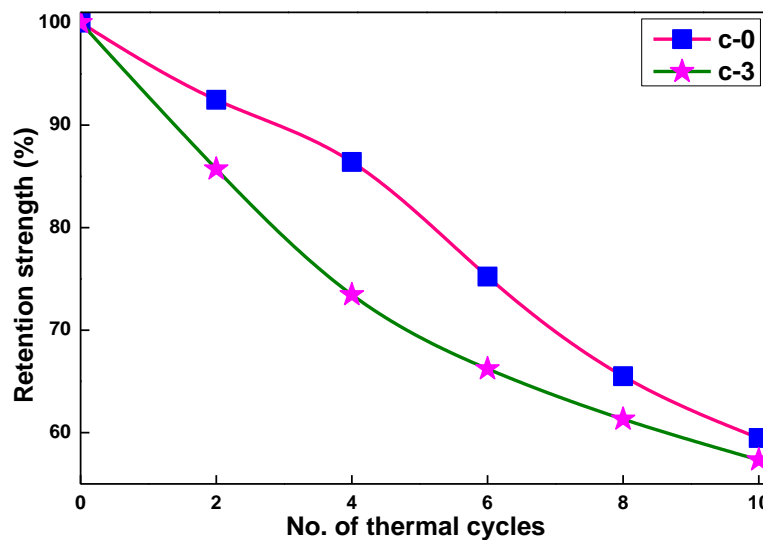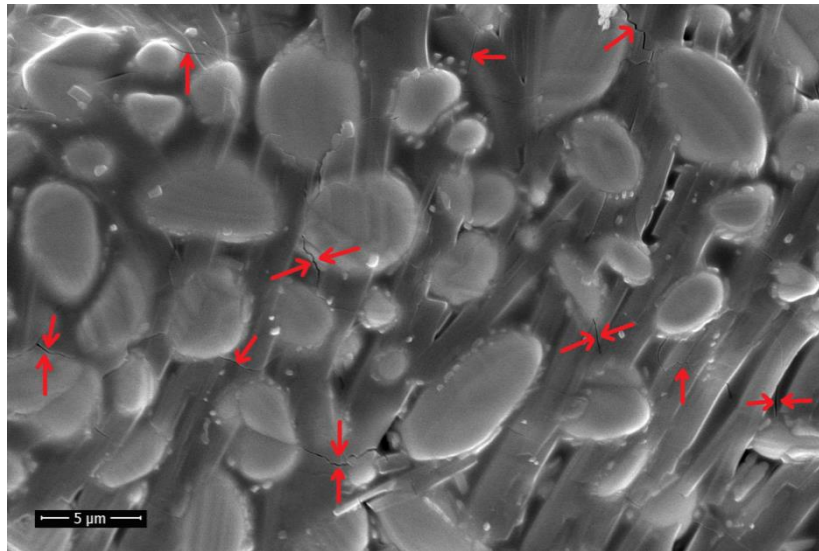**Figure 5.6** HMoR values of castable specimens at 1400°C.

**Figure 5.7** Retention of CCS values of c-0 and c-3 specimens after undergoing number of thermal cycle.

**Figure 5.8** SEM micrograph of s-3 specimen after 6th thermal shock.

c-3 specimen after firing at 1550°C is exhibited optimum properties without free silica among other sol containing specimens. This composition (c-3) and 4 wt.% CAC containing (c-0) specimen are selected for blast furnace slag (BFS) corrosion test. The composition of BFS is tabulated in Table 3.2. In the BFS, the major compounds are CaO, SiO_2 and Al_2O_3 with around 40.67 wt.%, 35.42 wt.% and 14.52 wt.%, respectively. BFS's melting temperature is above 1400°C. The corrosion test is performed at 1500°C for 30 h in an air atmosphere and the test schematic is represented in Figure 5.9. The corrosion region and the depth of slag penetration are observed by the SEM micrograph and EDX-mapping at castable-slag interface, as shown in Figure 5.10. c-0 sample exhibits a clear corrosion region in the interface of castable-slag. The presence of fused phases at high temperature have been reacted more potentially with the slag melt and permitted to the slag penetration in the castable. The liquid phases are unable to build the barrier for slag penetration. Therefore, different ions from slag easily transfer into castable. EDX-mapping image for c-0 (Figure 5.10) shows the Ca ion migration from the slag to castable. It is clearly observed that the ion concentration of Ca in the corrosion region is higher than non-corrosive region in the castable. The slag penetration depth of c-0 sample is around 150 μm after 30 h of heat-treatment. Oppositely, c-3 shows a superior corrosion resistance behavior due to highly dense microstructure (Figure 5.3) and phase purity (Figure 5.2). The absent of any low melting phases like free silica helps

[81]

to enhance the slag corrosion resistance. Additionally, the formation of in-situ mullite phase (~17.75 wt.% theoretically) in the system retains the orthorhombic crystal structure, which has oxygen vacancies and it is capable to arrest many cations like Mg, Ti, Fe, etc. (Singh and Sarkar, 2016). Many cations from the slag melt are diffused into the developed in-situ mullite and therefore, viscosity and composition of the slag is changed. It is resulted in the further reduction of slag penetration (Singh and Sarkar, 2016). Therefore, c-3 specimen shows the low density of Ca ion concentration (Figure 5.10) in the castable and the depth of penetration is around ~65 μm.
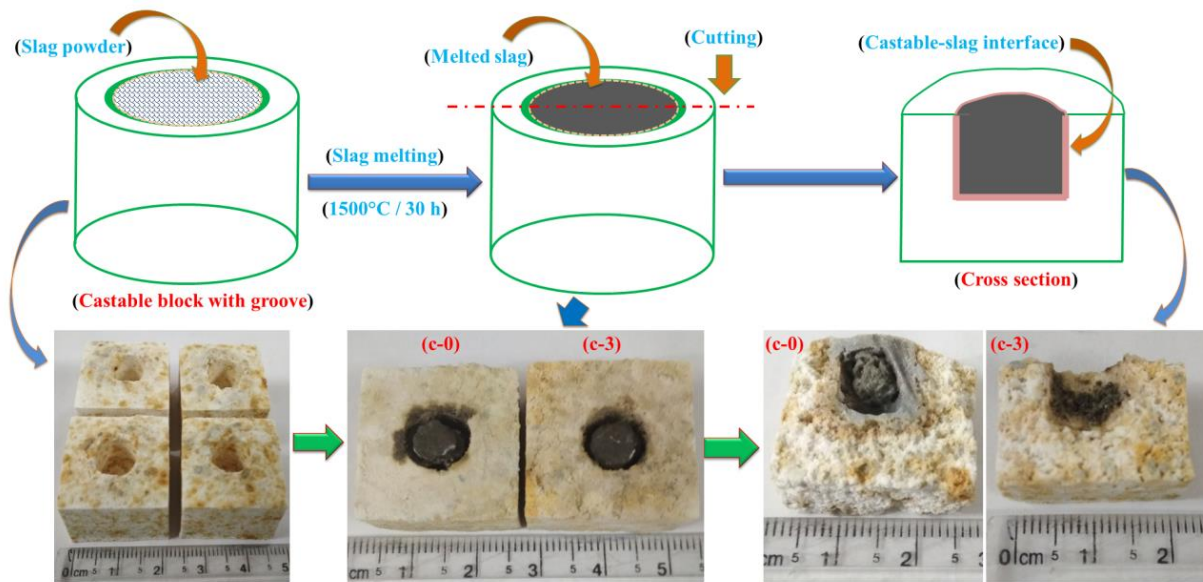
Figure 5.9 Schematic representation of static corrosion test.
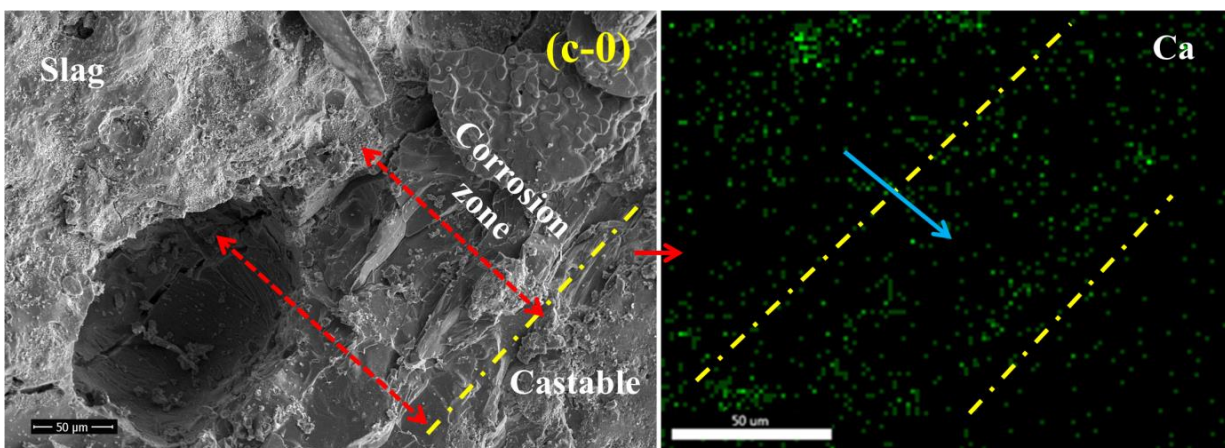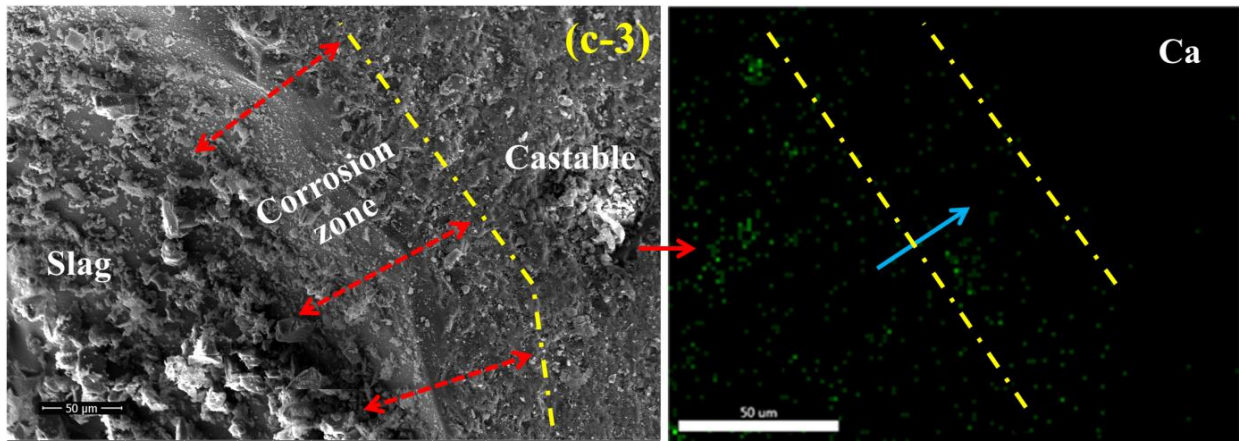
Figure 5.10 SEM photomicrographs and EDX-mapping analysis of the castable-slag interface after BFS corrosion test.

The comparable studies on the different properties of waste RHA derived sol bonded castable (c-3) with convention silica bonded systems are shown in Table 5.4. Though, the composition of refractory aggregates, different additives and particle size distribution are not same with this study. It can be observed that evaluated properties of c-3 sample are suitable according to the other sources of silica bonded castables. Thus, waste RHA derived sol has been a great potential as a sustainable source of silica sol for replacing the conventional silica sources in cement free unshaped refractory.

Table 5.4 Physico-mechanical properties of waste RHA derived sol bonded castable against other source of silica sol bonded castables.

Properties	Our study (c-3)	Colloidal silica (Singh and Sarkar, 2017)	Silica sol (Qiu et al., 2018)	Colloidal silica (Luz et al., 2018)
Firing temperature (°C)	1550	1600	1650	1400
Bulk density (gm/cc)	2.91	3.05	3.17	-
Strength after fired (MPa)	88 (CCS), 64 (BS)	110 (CCS)	27 (BS)	32 (BS)
HMoR at 1400°C (MPa)	14	9	-	10
TSR after 8th cycle (MPa)	53	64	-	-

5.4 Summary

Stable silica sol is prepared from waste RHA through the alkali extraction route. The sol contained 30 wt.% of nano amorphous silica with an average particle size 22 nm, and the estimated cost of per litre sol is around 9.35 $. No cement high alumina refractory castable specimens are prepared by the replacing of calcium alumina cement through the RHA derived

sol. Densification, cold and hot strength and corrosion resistance of the castable specimens are improved with the incorporation of sol. Sol containing nano silica is reacted with different alumina sources in the castable and started formation of in-situ mullite at above 1200°C. 5 wt.% (c-3) silica containing 1550°C sintered sample shows good physico-mechanical properties without retaining unreacted free silica. The evaluated properties of castable are compared with the convention colloidal silica bonded castable, and good matching is observed. The absence of any liquid phase formation (free silica) and superior properties of waste derived sol containing cement free castable system is able to be useful for high temperature applications like steel ladles and blast furnaces lining.